Multivariable Steffensen's Accelerator in Adaptive Sliding Mode Control

Awudu Atinga

Doctoral School of Applied Informatics and Applied Mathematics, Obuda University Bécsi út 96/B, H-1034 Budapest, Hungary.
UGN9N8.uni-obuda.hu@stud.uni-obuda.hu

Krisztián Kósi

John von Neumann Faculty of Informatics, Obuda University Bécsi út 96/B, H-1034 Budapest, Hungary.
kosi.krisztian@nik.uni-obuda.hu

József K. Tar

University Research and Innovation Center, Obuda University Bécsi út 96/B, H-1034 Budapest, Hungary.
tar.jozsef@nik.uni-obuda.hu

Abstract: Due to their internal mathematical structure Sliding Mode Controllers (SMC) are robust against the imprecisions of the dynamic model they use for the calculation of the necessary control forces as well as against a priori not known external disturbances. However, this robustness has natural limits. To widen the range of stable operation various particular constructions have been developed and tested in the recent decades. Key element of stability is the more or less precise realization of the invented kinematic design. To guarantee that natural possibility seems to be the integration of SMC technique with adaptive ones that also aim at the precise realization of the kinematic designs in the possession of some available, normally imprecise dynamic model. Due to its simple mathematical structure the Fixed Point Iteration (FPI)-based adaptive control seems to be a good candidate for this purpose. Like the SMC control, FPI-based adaptive controllers also suffer from certain limitations due to which they cannot be considered as some "panacea" against modeling errors. They work on the basis of iterative sequences generated by a contractive map in a Banach space, and their speed of convergence is limited by the fact that during one digital control step only one step in this iteration can be executed. Beside decreasing the cycle time of the digital control this convergence can be speeded up by a witty trick suggested by Steffensen in 1936 for single variable functions. In this paper it is shown how Steffensen's convergence accelerator can be generalized for *multiple variable Banach sequences. Following that simulation results are presented that testify that the simplest SMC and the simplest variant of the FPI-based adaptive controller using Steffensen's generalized accelerator can be successfully integrated in the precise control of a strongly nonlinear benchmark system consisting of two nonlinearly coupled generalized van der Pol oscillators. Robustness of the integrated controller is also tested against the modification of the control parameters. Furthermore, it is shown that the sensitivity of the control to the measurement noise efficiently can be reduced by reducing the cycle time of the digital control.*

Keywords: Sliding Mode Control, Fixed Point Iteration-based Adaptive Control, Banach Sequences, Steffensen's Convergence Accelerator.

1 Introduction

Control systems can be modeled mathematically by coupled nonlinear differential equations. Nonetheless, these models may contain errors that can negatively impact the controlled system's performance. Therefore, it is essential to consider these inaccuracies while designing control systems. The most widely used approaches for addressing these inaccuracies are *robust* and *adaptive* ones. These approaches compensate for the model's inaccuracies and ensure that the control system performs more precisely [1, 2].

In general, in the robust technology outlined in [1] the controlled system may chatter that practically must be avoided because it destroys its drive system and can excite not modeled internal degrees of freedom similarly to some resonance effect. A brief survey on the technologies that were elaborated to further develop the Robust Variable Structure/Sliding Mode (VS/SM) technology will be given in Section I.1

This study proposes a new design approach to reduce or eliminate chattering in controlled systems. It applies Fixed Point Iteration (FPI)-based adaptive control, namely the Robust Fixed Point Transformation (RFPT) control framework [3] to precisely realize the kinematically designed sliding mode controller. Furthermore, it applies a generalized version of Steffensen's original convergence accelerator [4] to achieve even more precise trajectory tracking than that available by the simple iterative adaptive control considered in [5].

In this paper at first the details of the suggested control are expounded, then Steffensen's convergence accelerator is briefed as it was originally elaborated for a single variable system. Following that Steffensen's method is generalized for multiple variables systems. To demonstrate the potential efficiency of the VS/SM technology improved with the accelerated FPI/RFPT-based adaptation the dynamic model of two modified, nonlinearly coupled van der Pol Oscillator is discussed. This strongly nonlinear system is used as a benchmark to produce simulation results. Robustness of the integrated method against the modification of the control parameters are also investigated. The paper is completed with a section of conclusions.

1.1 THE CLASSIC SLIDING MODE CONTROLLER

The Sliding Mode Controller can be regarded as a modification of the special version of the simplest model-based controller, the Computed Torque Control developed for robots (e.g., [6]), in which the dynamic model of a second order system and its inverse in the form of (1)

$$\ddot{q}=\Phi(q,\dot{q},Q) \quad , \quad Q=\Psi(q,\dot{q},\ddot{q}) \tag{1}$$

are directly utilized for the calculation of the necessary control forces $Q(t)$ ($q(t)$ denotes the *generalized coordinate* of the controlled system). Normally there is an *a priori known nominal trajectory* to be tracked, i.e., $q^N(t)$, while the actual trajectory is $q(t)$. The tracking error is their difference that mainly originates from the differences in the initial conditions. If the inverse model in (1) is precise, the following kinematic strategy, based on the tracking error, its time-integral, and time-derivative

$$e(t):=q^N(t)-q(t)\ ,\ e_{\text{int}}(t):=\int_{t_0}^{t} e(\xi)d\xi \tag{2}$$

can be realized:

$$\left(\Lambda+\frac{d}{dt}\right)^2 e_{\text{int}}(t)\equiv 0 \text{ leading to} \tag{3a}$$

$$\ddot{q}^{Des}(t)=\ddot{q}^N(t)+\Lambda^3 e_{\text{int}}(t)+3\Lambda^2 e(t)+3\Lambda\dot{e}(t) \tag{3b}$$

in which the feedback gains of the integrated error, the error, and its time-derivative are calculated from a single positive constant, $\Lambda>0$. Since the general solution of the equation $\left(\Lambda+\frac{d}{dt}\right)f(t)=0$ is $f(t)=\exp(-\Lambda(t-t_0))f(t_0)$ that converges to 0 as $t\to\infty$, from (3a) it evidently follows that $\left(\Lambda+\frac{d}{dt}\right)^2 e_{\text{int}}(t)$ as well as $\left(\Lambda+\frac{d}{dt}\right)e_{\text{int}}(t)\to 0$ as $t\to\infty$ that implies that $e_{\text{int}}(t)\to 0$ as $t\to\infty$. Since

$$\left(\Lambda+\frac{d}{dt}\right)^2 e_{\text{int}}(t)=0 \text{ leads to} \tag{4}$$

$\left(2\Lambda+\frac{d}{dt}\right)e(t)=-\Lambda^2 e_{\text{int}}(t)$, from which, after vanishing the inhomogeneous term at the right hand side, $e(t)\to 0$ as $t\to\infty$ can be concluded. In similar manner (3a) can be rewritten as

$$\left(3\Lambda+\frac{d}{dt}\right)\dot{e}_{\text{int}}(t)=-\Lambda^2 e_{\text{int}}(t)-3\Lambda^2 e(t) \tag{5}$$

in which the inhomogenous term vanishes again, therefore $\dot{e}(t)\to 0$ as $t\to\infty$ can be concluded.

Simulation results as well as practical experiences have shown that precise realization of the kinematic strategy in (3) requires quite precise dynamic model that normally is not available (e.g.,[7, 8]). To tackle this problem the basic idea was introduction of the *error metric* as

$$S(t)\overset{def}{=}\left(\Lambda+\frac{d}{dt}\right)^2 e_{\text{int}}(t) \ , \tag{6}$$

and instead of prescribing the precise damping for the tracking error in (3a) it is required to drive $S(t)$ during finite time near zero, and afterwards keeping it in the vicinity of zero, e.g., by approximating the strategy given in (7)

$$\frac{dS(t)}{dt}=-K\tanh\left(\frac{S}{w}\right) \ , \tag{7}$$

in which the constant parameter $K>0$ determines the speed of damping $S(t)$, and $w>0$ is the smoothing parameter that determines the nature of the motion near $S=0$ (e.g., [1]). The main point is that *no precise realization* of (7) is *necessary*. From $S(t)\approx 0$, similarly to the consideration made for (3a) $e_{\text{int}}(t)\to 0$, and $e(t)\to 0$ can be concluded, but generally nothing can be stated about the behavior of $\dot{e}(t)$. It can take huge values even for quite small $e(t)$ errors (this is the phenomenon referred to as *chattering*), or can be nicely limited, depending on the modeling errors, and the parameters K and w. While Λ and K mainly are responsible for the tracking error, W can be set to avoid chattering. Since greater w keeps $S(t)$ less precisely around zero, increasing its value normally makes the tracking less precise. The inherent *robustness* of the method consists in the fact that a very precise realization of (7) would require a precise dynamic model, however, its exact realization practically is out of interest.

Evidently, (7) is not the only kinematically formulated strategy that can satisfy the goals to push S during finite time to zero then keeping the physical state of the system creeping in the vicinity of the hypersurface $S\simeq 0$. Already in the past Soviet Union the idea was extended to higher order dynamical systems as supervision of rough bang-bang control (e.g., [9]– [11]). According to the actual kinematic prescriptions the controlled system receives a drastic “flap” from the controller whenever its error metric crosses the $S \equiv 0$ hypersurface. In this technology the crucial aspect is appropriate timing of the “flaps” (e.g., [12, 13]). Due to its robustness, fast error convergence, and dynamic response, the sliding mode method has obtained significant attention in developing controllers for robotic manipulators, underwater vehicles, automotive transmissions and engines, high-performance electric motors, and power systems (e.g., [14]).

Various methods were suggested that tried to decrease or eliminate the reaching phase of $S = 0$ to minimize the system’s parameter sensitivity. Among these methods, one involves modifying the sliding surface of classical SMCs, which are naturally linear and constant. The system’s performance is determined by the design of the sliding surface, making it the focal point of most robust control strategies (e.g., [15]).

The idea of chattering reduction by “smoothing” the signum function (i.e., replacing it with some saturation function) in the switching rule similar to (7) was suggested in [16]. To further reduce chattering, a Recurrent Elman Neural Network (RENN) was constructed to determine the switching gain.

A possible method to avoid chattering is using a dead band or boundary layer in a tight neighborhood of the sliding surface [17]. In [18], boundary layers are employed near the sliding surface to implement continuous control within the boundary. The paper also discusses the effect of different controls within the boundary layer on chattering and error convergence in various systems. Also, in [19], discontinuous control is used outside the boundary layer and then switches to uncertainty and disturbance estimator (UDE) based control inside. The paper addresses the issue of sizable initial control underlying the method of UDE with a modified sliding surface. In [20], a control law is presented that incorporates a cone-shaped boundary layer around the sliding mode plane to eliminate chattering. This boundary layer combines two types: a constant layer and a sector-shaped layer. The system states will always enter the cone-shaped boundary layer, and the choice of the sliding mode will determine the system’s performance.

In many practical cases, in which the modeling errors are not critical, by well setting Λ, K, and w, quite acceptable results can be achieved by using the simple idea formulated in (7). However, the method is not a “panacea”, and too drastic errors cannot be well treated by it. In the lack of better dynamic model, beside the above mentioned more sophisticated and complex methodologies, a natural possibility is to combine this robust technique with some adaptive one to better approximate (7).

The design of adaptive techniques goes back to the nineties of the past century [2] when formally correct dynamic models having imprecise parameters were used as a starting point then the system learned the precise parameter values by a tuning process based on Lyapunov's 2nd method [21, 22]. This technique can be regarded a prevailing design concept in or days, too. After inventing the concept of "universal approximators" (Weierstraß' polynomials in 1885 in [23], the generalization of this idea by Stone in 1948 [24], the construction method of making multiple variable continuous functions from single variable ones by Kolmogorov in 1957 [25], Sprecher and Lorentz in the sixties in [26, 27], the concept of fuzzy sets by Zadeh in 1965 in [28]), a new trend was initiated in which huge universal structures having plenty of free parameters that are tuned by some nature-inspired method as Genetic Algorithm yields the solution even for relatively simple dynamical systems (e.g., the "ball on the wheel system" in [29]). Special model forms as the Linear Parameter Varying models (e.g., [30]) are applied in [31] in the cruise control of autonomous cars. The adaptation mechanism can be based on learning control as e.g., in [32]. It was Weierstraß who made the first pioneering step towards the understanding of the incredible complexity by modeling with continuous functions by giving an example that is an everywhere continuous function that nowhere is differentiable in 1872 in [33]. A plausible possibility is the implementation of this robust technique in the Adaptive *Fixed-Point Transformation* (RFPT) digital control framework that is the simplest adaptive technique. It is briefed in the sequel.

1.1.1 ON THE FIXED POINT ITERATIONS-BASED ADAPTIVE CONTROL.

The basic idea of the method at first published in [3] is very simple. Let us return to (1) in which $\Phi(q,\dot{q},Q)$ is precisely realized by the physics of the controlled system while the inverse model is only approximately known as $Q=\tilde{\Psi}(q,\dot{q},\ddot{q}^{Des})$, in which the *desired 2nd time-derivative* $\ddot{q}^{Des}$ is computed from (7). Evidently, *the realized 2nd time-derivative* $\ddot{q}(t)$ will be

$$\ddot{q}^{Des}\neq\ddot{q}=\Phi\left(q,\dot{q},\tilde{\Psi}(q,\dot{q},\ddot{q}^{Des})\right)\approx f(\ddot{q}^{Des}) \tag{8}$$

where it was taken into account that $\dot{q}$ and q can only vary slowly, while $\ddot{q}$ can be drastically and abruptly changed by abrupt changes in the control force. The *response function* defined in (8) slowly can drift with $q(t)$ and $\dot{q}(t)$. To compensate for the effects of the modeling errors the idea arose that it would be expedient to find some *deformed* $\ddot{q}^{Def}$ value and placing it into the approximate inverse dynamic model to achieve the situation $\ddot{q}=\ddot{q}^{Des}=f(\ddot{q}^{Def})$. In this case (7) would be precisely realized. For finding the necessary deformation, in the case of a digital controller an iteration was suggested so that during each digital control step only one step of the adaptive iteration can be done. For this purpose a *deformation function* in (9)

$$\ddot{q}^{Def}(i+1)=G\left(\ddot{q}^{Def}(i),\ddot{q}(i),\ddot{q}^{Des}(i+1)\right) \tag{9}$$

was suggested with the physical interpretation as follows: for the calculation of the deformed value in the cycle $i+1$, i.e., $\ddot{q}^{Def}(i+1)$, in which the desired value is $\ddot{q}^{Des}(i+1)$, the observed effect (i.e., $\ddot{q}(t)$) of the previously applied deformation $\ddot{q}^{Def}(i)$ is taken into account. In the above approximation G contains the *response function* in the form $G(\ddot{q}^{Def}(i), f(\ddot{q}^{Def}(i)), \ddot{q}^{Des}(i+1))$. This function must be so constructed that the appropriate deformation , i.e., the solution of the control task, $\ddot{q}_*^{Def}$ must be its *fixed point* as $\ddot{q}_*^{Def} = G(\ddot{q}_*^{Def}(i), f(\ddot{q}_*^{Def}), \ddot{q}^{Des})$ for a constant $\ddot{q}^{Des}$. For constructing such a function various possibilities exist. Perhaps the simplest idea is based on a constant $\alpha > 0$ parameter and direct use of the response function in the iterative sequence in the vicinity of the desired solution $f(x_*) = x^{Des}$ as

$$x_{i+1} = x_i + \alpha(x^{Des} - f(x_*)) \ , \tag{10}$$

in which the correction happens in the direction that connects the desired value with the last obtained response. For a differentiable response function in the vicinity of the solution it can be written that

$$f(x) \equiv f(x_* + x - x_*) \simeq x^{Des} + \frac{\partial f}{\partial x}\Big|_{x_*}(x - x_*) \ , \tag{11}$$

that simply leads to

$$x_{i+1} - x_* \approx \left[I - \alpha \frac{\partial f}{\partial x}\Big|_{x_*} \right](x_i - x_*) \ , \tag{12}$$

from which it follows that

$$\begin{aligned} \|x_{i+1} - x_¿\|^2 \approx \|x_i - x_*\|^2 - \alpha(x_i - x_*)^T \left(\frac{\partial f^T}{\partial x} + \frac{\partial f}{\partial x} \right)(x_i - x_*) \\ + \alpha^2 (x_i - x_*)^T \frac{\partial f}{\partial x}^T \frac{\partial f}{\partial x}(x_i - x_*). \end{aligned} \ , \tag{13}$$

In (13) the last term is always positive but for small enough α it can be neglected in comparison with the first order term in α. In [34] as the generalization of the *monotonic increasing single variable function* the concept of the *locally approximately direction keeping multivariable function* was defined as follows:

$$\Delta x^T \Delta f \equiv \Delta x^T (f(x + \Delta x) - f(x)) \approx \Delta x^T \frac{\partial f}{\partial x} \Delta x > 0 \ , \tag{14}$$

that simply means that the scalar product of the vectors Δx and Δf is positive, that is the angle between these vectors is *acute*, i.e., these vectors approximately have the same direction. By decomposing the matrix $\frac{\partial f}{\partial x}$ into its *symmetric* and *skew symmetric* parts the above definition means that

$$\begin{aligned}&\Delta x^T\left[\frac{1}{2}\left(\frac{\partial f}{\partial x}+\frac{\partial f}{\partial x}\right)+\frac{1}{2}\left(\frac{\partial f}{\partial x}-\frac{\partial f}{\partial x}^T\right)\right]\Delta x=\\&\Delta x^T\frac{1}{2}\left(\frac{\partial f}{\partial x}+\frac{\partial f}{\partial x}^T\right)\Delta x>0,\end{aligned} \quad , \tag{15}$$

since due to symmetry reasons the contribution of the skew symmetric part is exactly 0. Therefore in (13) it can be achieved that for a small positive $\alpha>0$ $\|x_{i+1}-x_*\|<\|x_i-x_*\|$, i.e., the iteration goes closer to the solution x_*. At this point Banach's fixed point theorem can be referred to from 1922 [36]: if a *contractive map over a Banach space (i.e., linear, normed, complete metric space* B) $\Phi:B\mapsto B$ generates a sequence as $\{x_0,x_1=\Phi(x_0),\ldots,x_{n+1}=\Phi(x_n),\ldots\}$ it converges to the unique fixed point of this map defined as $\Phi(x_*)=x_*$. By definition $\Phi(x)$ is *contractive* if $\exists 0\le K<1$ so that $\forall y,x\in B$ $\|\Phi(y)-\Phi(x)\|\le K\|y-x\|$. On this basis it can be expected that for many physical systems with their approximate models convergent iteration can be obtained. Since in the practice it is difficult to estimate the appropriate α that keeps fast enough convergence, various G deformation functions were elaborated for use in (9). In [35] this parameter was replaced with another one that must be located in the (0, 1] interval. Earlier in [36] a different solution was suggested that practically used a single parameter, and originally in [3] a solution was given that used three real parameters $(K_c, B_c$ and $A_c)$ for single variable functions, the Robust Fixed Point Transformation, that was defined as follows:

$$\ddot{q}^{Def}(i+1)=(\ddot{q}^{Def}(i)+K_c)\left[1+B_c\tanh(A_c(\ddot{q}(i)-\ddot{q}^{Des}(i+1)))\right]-K_c\ . \tag{16}$$

These parameters were set in the following manner: after making simulations for the non-adaptive PID-type CTC controller a great positive $K_c>>|\ddot{q}|$ was chosen. By trying to set $B_c=\pm 1$ a small $A_c>0$ was chosen to achieve convergence in the adaptive simulations. In the present simulations a primitive generalization of (16) will be applied: it must be valid for each component of $\ddot{q}\in\Re^n$.

According to simulation investigations (16) worked well in the solution of certain adaptive control solutions, but in other cases problems arose with the speed of convergence with a fixed parameter set. So this adaptive solution is not a "panacea" in the adaptive PID-type CTC control, similarly to the simple SMC control in (7) with its fixed parameters. The idea of combining the two methods naturally arises. Before doing that it is expedient to consider the possibilities for speeding up the convergence of the fixed point iteration-based approach, because during one digital control step only one iterative step can be realized. In this direction Steffensen made the pioneering work for single variable functions. In the sequel its original idea is briefed then its generalization to multiple variable functions will be presented.

1.1.1 STEFFENSEN'S CONVERGENCE ACCELERATOR

This method was invented in 1933 in [4] for speeding up the convergence of single variable sequences generated by a *contractive map over a Banach space* $\Phi : B \mapsto B$ as $\{x_0, x_1 = \Phi(x_0), \ldots, x_{n+1} = \Phi(x_n), \ldots\}$ that according to Banach's fixed point theorem converges to the unique fixed point of this map $\Phi(x_*) = x_*$ [36]. By definition $\Phi(x)$ is contractive if $\exists 0 \leq K < 1$ so that $\forall y, x \in B \quad \|\Phi(y) - \Phi(x)\| \leq K \|y - x\|$. The speed of convergence can be estimated by the parameter K and it can be quite slow if it is close to 1.

A The Single Variable Case

Steffensen realized that it is expedient to break the infinite sequence into finite number excerpts as $\{x_0, x_{n-1} = \Phi(x_0), x_n = \Phi(x_{n-1}), x_{n+1} = \Phi(x_n)\}$ in which x_0 does not originate as a function of a previous point of the sequence. Instead of that, in the vicinity of the fixed point the derivative of $\Phi(x)$, i.e., $\Phi'(x)$ can be estimated as

$$\Phi'(x) \approx \frac{\Phi(x_n) - \Phi(x_{n-1})}{x_n - x_{n-1}} = \frac{x_{n+1} - x_n}{x_n - x_{n-1}} , \tag{17}$$

and in first order Taylor estimation , instead of generating $x_{n+2} = \Phi(x_{n+1})$ of the Banach sequence immediately try to find the fixed point as $\Phi(x_{n+1} + \Delta x) = x_{n+1} + \Delta x \approx x_*$ that with the above estimation of the derivative leads to the approximation

$$x_{n+1} + \Delta x = x_{n+1} + \frac{(x_{n+1} - x_{n+2})(x_n - x_{n-1})}{x_{n+1} - 2x_n + x_{n-1}} \quad . \tag{18}$$

This value will be the initial element of the next excerpt of the sequence that can be written into the next starting variable x_0. To avoid division by zero by the introduction of the small positive constant $0 < \varepsilon$ the following approximation can be done:

$$x_0 \approx x_{n+1} + \frac{(x_{n+1} - x_{n+2})(x_n - x_{n-1})(x_{n+1} - 2x_n + x_{n-1})}{\varepsilon + (x_{n+1} - 2x_n + x_{n-1})^2} . , \tag{19}$$

In the case of the digital controller it must be taken into account that the response functiom's values are not known in advance: they are obtained via observations with a fixed cycle time δt. Accordingly, a deformed sequence $\{\ddot{q}^{Def}(n)|n\in N\}$ is initiated $\ddot{q}^{Def}(1)=\ddot{q}^{Des}(1)$. The elements as $\{x_0, x_{n-1}=\Phi(x_0), x_n=\Phi(x_{n-1}), x_{n+1}=\Phi(x_n)\}$ can be refreshed as global variables in a sequential program code for simulation investigations.

B The Multiple Variable Case

Formally the idea could be applied if in the vicinity of the fixed point the Jacobian matrix $\frac{\partial \Phi}{\partial x}$ could be estimated for $x, \Phi \in \Re^n$. An equation

$$f(x_{i+1}+\Delta x)\approx f(x_{i+1})+\frac{\partial f}{\partial x}|_{x_*}\Delta x=x_{i+1}+\Delta x\ , \tag{20}$$

could be solved for Δx. However, in the case of a smooth motion there is no mode to estimate the Jacobian because for this purpose real time measurements should be made in essentially linearly independent directions. Fortunately in the case of a continous smooth function it is not necessary to obtain information on various directions. Again, the idea of *motion approximately in the same direction* can be introduced and utilized similarly as it was done in (14). Instead of going to point $x_{i+2}=\Phi(x_{i+1})$ introduce the unit vector $e_{i+1}\overset{def}{=}\frac{x_{i+2}-x_{i+1}}{\|x_{i+2}-x_{i+1}\|}$, and instead of estimating the Jacobian, *estimate its effect approximately in the same direction* as

$$\gamma\overset{def}{=}\frac{\|x_{i+2}-x_{i+1}\|}{\|x_{i+1}-x_i\|}\ , \tag{21}$$

and seek the appropriate Δx *appropriately in the same direction* as $\Delta x=\beta e_{i+1}$. For approximating the fixed point in this direction the equation

$$\Phi(x_{i+1}+\Delta x)\approx\Phi(x_{i+1})+\gamma\beta e_{i+1}=x_{i+1}+\beta e_{i+1}\ , \tag{22}$$

should be solved. Since $x_{i+2}=\Phi(x_{i+1})$ a consistent solution can be obtained as

$$\|x_{i+2}-x_{i+1}\|(x_{i+2}-x_{i+1})=\beta(1-\gamma)(x_{i+2}-x_{i+1})\ , \tag{23}$$

that can be solved for the vector $(x_{i+2}-x_{i+1})\neq 0$ leading to

$$\Delta x=\frac{\|x_{i+1}-x_i\|(x_{i+2}-x_{i+1})}{\|x_{i+1}-x_i\|-\|x_{i+2}-x_{i+1}\|}\ . \tag{24}$$

Again, to avoid division by 0 the trick using a small positive value $\varepsilon>0$ can be applied for the approximation of the fixed point as

$$\Delta x\approx(x_{i+2}-x_{i+1})\frac{\|x_{i+1}-x_i\|\left(\|x_{i+1}-x_i\|-\|x_{i+2}-x_{i+1}\|\right)}{\varepsilon+\left(\|x_{i+1}-x_i\|-\|x_{i+2}-x_{i+1}\|\right)^2}\ . \tag{25}$$

1.1.2 THE EFFECTS OF THE MEASUREMENT NOISE

By feeding back the observed $\ddot{q}(t)$value that normally is burdened by measurement noise, the FPI-based approach normally requires the application of a simple low pass filter as it was done e.g., by Bodó et Lantos in [37]. The main source of the noise normally is the imprecision of the measurement of the coordinates $q(t)$. In general it can be modeled by adding a random term to the exact coordinate value $q(t)$ so that the addition has Gaussian distribution with zero mean as

$$q_o(t)=q(t)+\aleph(t) \ . \tag{26}$$

that normally cause high frequency disturbance of which one can get rid by the application of a simple low pass filter that consists of an observer that follows the noisy signal with some "inertia" represented by the constant parameter $0<\Lambda_f$ as

$$\left(\Lambda_f+\frac{d}{dt}\right)^3 q_s(t)=\Lambda_f^3 q_o(t) \ . \tag{27}$$

For computing the filtered $q_o(t)$ determined by (27) in the time domain with the initial condition $q_o(t)=0$, $\dot{q}_o(t_0)=0$, and $\ddot{q}_o(t_0)=0$ the simple numerical Euler integration of the third order differential equation (28) can be done as

$$\dddot{q}_s(t)=\Lambda_f^3(q_o(t)-q_s(t))-3\Lambda_f^2\dot{q}_s(t)-3\Lambda_f\ddot{q}_s(t) \ . \tag{28}$$

Normally the assumption of the Gaussian distribution is proposed on the theoretical basis that the resulting distribution of infinite number of random external effects must be of Gaussian type. However, if the noise originates from the measuring imprecision of digital encoders, the even distribution within the bounded interval $[-\sigma,+\sigma]$ is a physically more realistic assumption (e.g.,[38]). The "delay" caused by the "inertia" of the noise filter considerably concerns the operation of the FPI-based control even if $\sigma=0$. In the sequel the dynamic model of the nonlinearly coupled van der Pol oscillators as a benchmark system is briefly presented.

1.1.3 THE DYNAMIC MODEL OF THE COUPLED VAN DER POL OSCILLATORS

In the simulations two modified van der Pol oscillators (the original version was published in [39]) was used that evolves according to the equation of motion the

$$\Im = k|q_1 - q_2|^{\nu} \operatorname{sign}(q_1 - q_2),$$
$$\ddot{q}_1 = \frac{u_1 + \mu_1 (a_1^2 - q_1^2)\dot{q}_1 - \omega_{1o}^2 q_1 - \alpha_1 q_1^3 - \lambda_1 q_1^3 - \Im}{m_1}.$$
$$\ddot{q}_2 = \frac{u_2 + \mu_2 (a_2^2 - q_2^2)\dot{q}_2 - \omega_{2o}^2 q_2 - \alpha_2 q_2^3 - \lambda_2 q_2^3 + \Im}{m_2} \tag{29}$$

where for oscillator i q_i [m] represents the position coordinate, u_i[N] denotes the control force, m_i[kg] is themass of the oscillator, and $0 < \mu_i$ is the scalar parameter that shows the damping strength. If $|q_i| < a_i$ the oscillator is excited (i.e., energy is added to the system), and if $|q_i| > a_i$, the oscillator is damped. Parameter $k\left[N \cdot m^{-\nu}\right]$ describes the strength, while ν [nondimensional] determines the nonlinearity of coupling. Letter $\Im$ denotes the coupling force. The dynamic model parameters used in the simulations are given in Table I.

TABLE 1

The dynamic model parameters used in the simulations

Model Parameter	**Exact Value**	**Approximate value**	**Physical Unit**
ν	1.5	2.0	[nondimensional]
k	80.0	60.0	$\left[N\cdot m^{-\nu}\right]$
a_1	0.5	0.8	$\left[m\right]$
a_2	1.5	1.0	$\left[m\right]$
μ_1	0.4	0.5	$\left[N\cdot m^{-3}\cdot s\right]$
μ_2	0.3	0.4	$\left[N\cdot m^{-3}\cdot s\right]$
ω_{1o}	0.46	0.42	$\left[N^{0.5}\cdot m^{-0.5}\right]$
ω_{2o}	0.40	0.32	$\left[N^{0.5}\cdot m^{-0.5}\right]$
α_1	1.0	0.9	$\left[N\cdot m^{-3}\right]$
α_2	1.2	1.0	$\left[N\cdot m^{-3}\right]$
λ_1	0.1	0.09	$\left[N\cdot m^{-5}\right]$
λ_2	0.2	0.1	$\left[N\cdot m^{-5}\right]$

For free oscillations, i.e., $u_i \equiv 0$, $\Im \equiv 0$, the state $q_i = 0, \dot{q}_i = 0$ corresponds to an unstable equilibrium point. However, if the system is moved out of this equilibrium point , it approaches a limit cycle corresponding to nonlinear oscillation.

1.1.4 THE SIMULATION RESULTS

The method intentionally was texted for a very drastic dynamic range caused by the strong nonlinear coupling in the two oscillators as given in Table I. In the simulation at first the SMC controller's parameters were set by applying various trials evaluating the improvement achieved in the phase trajectories in comparison with that of the simple non-adaptive PID-type CTC controller determined by $\Lambda = 0.5\,[s^{-1}]$. For noise reduction the constant $\Lambda_f = 1300.0\,[s^{-1}]$ was applied. The discrete time resolution and the cycle time of the adaptive controller was fixed cycle time $\delta t = 10^{-3}[s^{-1}]$. In the beginning no measurement noise was simulated.

Figure 1 reveals very imprecise phase trajectory tracking

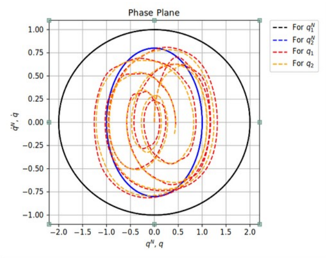

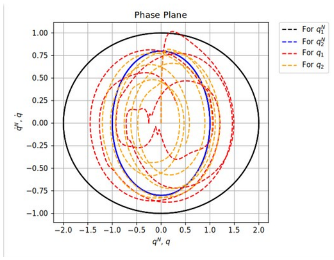

Figure 1
Phase trajectory tracking of the original PID controller without adaptivity, and simulated noise

Figure 2
Phase trajectory tracking of the simple SMC controller without adaptivity, and noise

Following that some SMC parameters were sought for. Without finding satisfactory solution the setting $K = 10^4\ [m \cdot s^{-2}] w = 600 [m \cdot s^{-1}]$ produced the result in Fig. 2 that revealvery little improvement in the phase trajectory tracking. It can be seen that no chattering occurred in the control. The trajectory tracking error is displayed in Fig. 3.

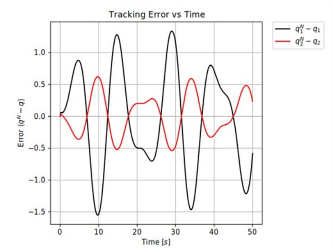

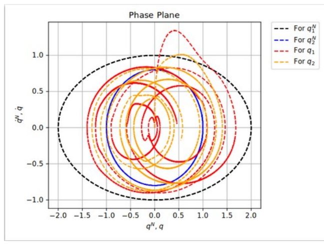

Figure 3
Trajectory tracking error of the simple SMC controller without adaptivity, and simulated noise

Figure 4
Phase trajectory tracking of the Adaptive SMC controller without Steffensen , and noise

In the next step the adaptive parameters were set via trials without using Steffensen's accelerator. It was found that the setting $K_c = 10^4 [m \cdot s^{-2}]$, $B_c = -1$ and $A_c = 0.15 / K_c$ for the adaptive control produced some little improvement in the phase trajectory tracking (Fig. 4). However, Fig. 5 shows little increase in the tracking error. Fig. 6 indicates that the applied parameter A_c was too great: instead speeding up the convergence the FPI-based control went out of its region of convergence and this fact caused the observable chattering.

The significance of guranteeing the necessary speed of convergence can be well revealed following switching on the generalized Steffensen's acclerator with its parameter $\varepsilon = 10^{-3}\,[m^2 \cdot s^{-4}]$ in Figs. 7 and 8. Considering Fig. 9 well illustrates the significance of this small tracking error. In Fig. 10 it definetely can be seen that the chattering disappeared. Figs. 11 and 12 show that very drastic extent of adaptive deformation was necessary to well approximate the prescribed nominal motion.

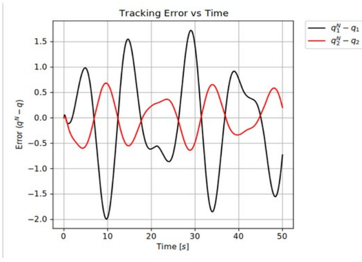

Figure 5

Trajectory tracking error of the adaptive SMC controller without Steffensen, and simulated noise

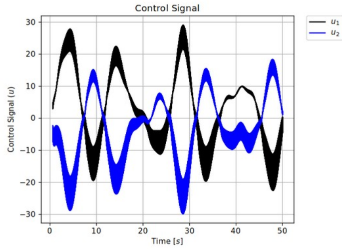

Figure 6

Control force of the Adaptive SMC controller controller without Steffensen , and noise

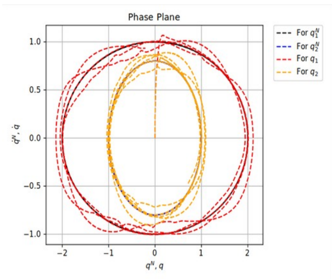

Figure 7

Phase trajectory tracking of the adaptive SMC controller with Steffensen, and without noise

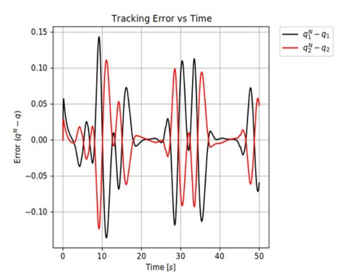

Figure 8

Trajectory tracking error of the Adaptive SMC controller with Steffensen , and without noise

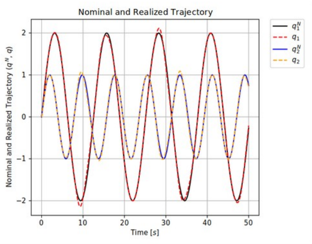

Figure 9
Trajectory tracking of the adaptive SMC with Steffensen accelerator, and without simulated noise

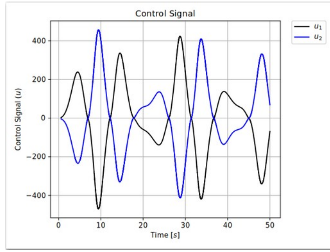

Figure 10
Control force of the Adaptive SMC controller with Steffensen's accelarator, and without simulated noise

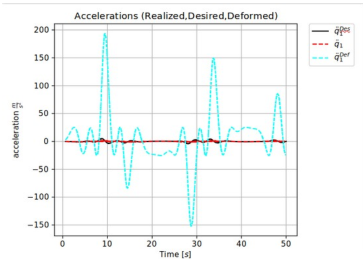

Figure 11
The $\ddot{q}_1(t)$ second time-derivatives in the adaptive SMC controller with Steffensen's accelerator , and without simulated noise

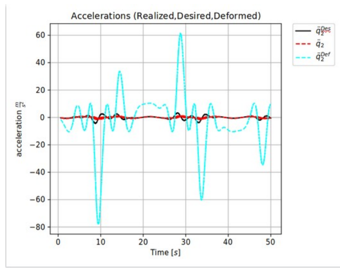

Figure 12
The $\ddot{q}_2(t)$ second time-derivatives in the adaptive SMC controller with Steffensen's accelerator, and without simulated noise.

To the effects of measurement noise some realistic noise distribution was chosen. In the Web various linear magnetic encoders can be found for measuring q_1 and q_2. For instance in

"https://www.rls.i/eng/la11-linear-absolute-encoder"

the "LA11 Linear Absolute Magnetic Encoder " is advertised with resolutions up to 0.244$[\mu m]$ that corresponds to $\sigma = 0.488 \cdot 10^{-6} \approx 5 \cdot 10^{-7}$ [m] even distribution. To the category of "High accuracy Linear Magnetic Encoder System" resolutions down to 0.1$[\mu m]$belong to industrially advertised items.

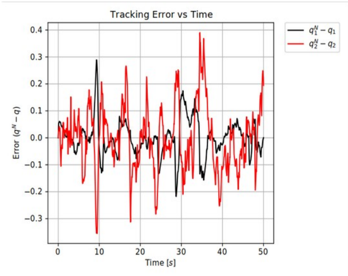

Figure 13
Trajectory tracking error of the adaptive SMC controller controller with Steffensen accelerator, and simulated noise of $\sigma = 5 \times 10^{-7}$ [m]

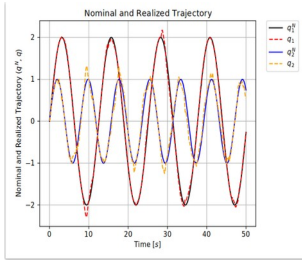

Figure 14
Trajectory tracking of the Adaptive SMC controller with Steffensen's accelarator, and simulated noise $\sigma = 5 \times 10^{-7}$ [m]

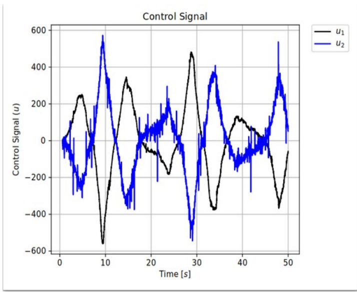

Figure 15
Control force of the Adaptive SMC controller with Steffensen's accelerator, and with simulated noise $\sigma = 5 \times 10^{-7}$ [m]

Figs. 13, 14, and 15 well illustrate that this order of magnitude noise cannot destroy the controller. Certain random fluctuation necessarily appears in the control forces because they are calculated by the use of noisy feedback terms in spite of the action of the noise filters.

On the basis of the symmetry in the driving force pictures (Figs 6, 10, and 15) it can be guessed that the main dynamice effect originated from the coupling force between the oscillators. Robustness of the suggested simple adaptive method can be tested for a model in which the coupling forces coefficient (parameter k in Table 1) is drastically decreased (naturally together with its approximate value) to allow the manifestation of the effects governed by the other nonlinear model parameters.

1.1.5 ROBUSTNESS TEST BY CONSIDERING WEAKENED NONLINEAR COUPLING BETWEEN THE OSCILLATORS

In the following simulations the exact value of the coupling parameter $k=0.5$ $[N \cdot m^{-\nu}]$ instead of that given in Table 1. Its approximate value was $1.0[N \cdot m^{-\nu}]$. For setting the SMC control parameters the same consecutive steps were done as in the strongly coupled case.

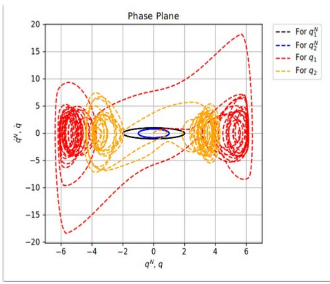

Figure 16

Phase trajectory tracking of the original PID controller without adaptivity, and simulated noise in the case of weak coupling

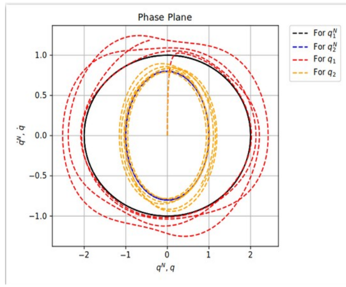

Figure 17

Phase trajectory tracking of the simple SMC controller without adaptivity, and simulated noise in the case of weak coupling

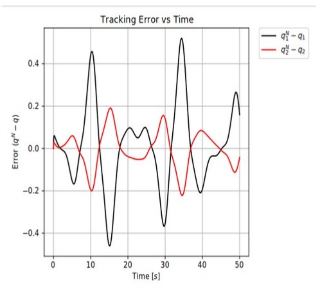

Figure 18

Trajectory tracking error of the simple SMC controller without adaptivity, and simulated noise in the case of weak coupling

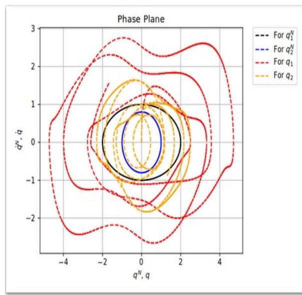

Figure 19

Phase trajectory tracking of the adaptive SMC controller without Steffensen's accelerator, and simulated noise in the case of weak coupling

Figure 16 in comparison with Fig. 1 reveals that these parameter estimation errors caused quite complicated phase tracking pattern in the simple non-adaptive PID-type control. Fig. 17 testifies that in this case switching on the simple SMC control without adaptation resulted in much better phase trajectory tracking. For further comparison the appropriate tracking errors are given in Fig. 18.

Figs. 19 and 20 show that something similar happened than in the case of strong coupling: without Steffensen's accelerator both of the phase trajectory tracking and the trajectory tracking error were worsened. Fig. 21 shows a little chattering that was cause by the too great parameter A_c. This conclusion is confirmed by the figures of the second time-derivatives (Figs. 22, 23), too.

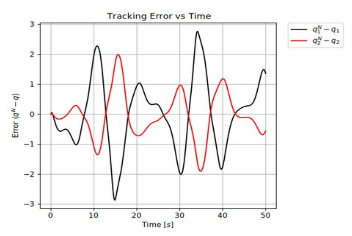

Figure 20

Trajectory tracking error of the adaptive SMC controller without Steffensen's accelerator, and noise in the case of weak coupling

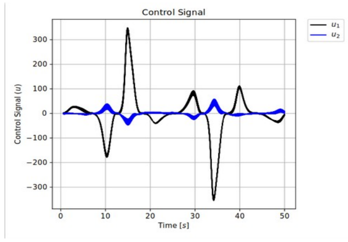

Figure 21

Control force of the adaptive SMC controller without Steffensens accelerator, and simulated noise in the case of weak coupling

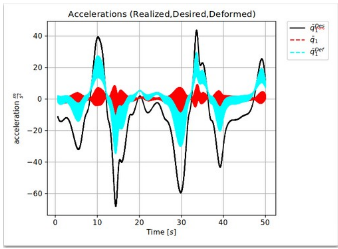

Figure 22

The $\ddot{q}_1(t)$ second-order derivative in the adaptive controller without Steffensen's accelerator, and simulated noise in the case of weak coupling

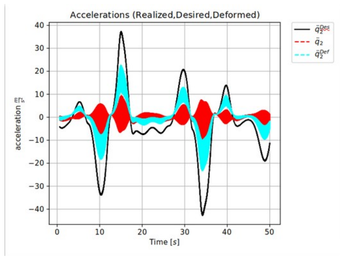

Figure 23

The $\ddot{q}_2(t)$ second-order in the adaptive SMC SMC without Steffensens accelerator, and simulated noise in the case of weak coupling

The previously observed "symmetry" disappeared in the graph of the control forces indicating that the dynamic details were mainly determined by the internal parameters of the coupled oscillations and the dynamic coupling between them played less significant role. In comparison with Figs. 11 and 12 of strong coupling it definitely can be stated that the extent of the necessary adaptive deformation was considerably smaller in the case of weak coupling.

Finally Steffensen's generalized accelerator was switched on with the same parameter $\varepsilon = 10^{-3} [m^2 \cdot s^{-4}]$. Figs. 24, 25, and 26 testify that very precise trajectory tracking was achieved. Comparison of Figs. 10 and 27 confirm that the reduction of the extent of dynamic coupling considerably reduced the necessary control forces. Also, comparison of Figs. 28, 29 and 11, 12 reveals that the extent of the necessary adaptive deformation was considerably reduced by weakening the dynamic coupling between the subsystems.

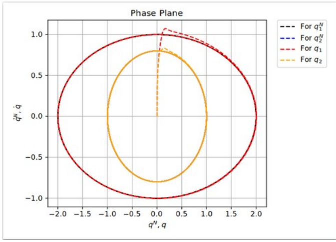

Figure 24
Phase trajectory tracking of the adaptive SMC controller with Steffensen's accelerator, and without noise in the case of weak coupling

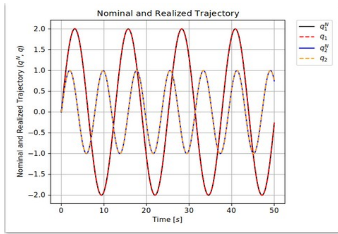

Figure 25
Trajectory tracking of the adaptive SMC controller controller with Steffensens accelerator, and without noise in the case of weak coupling

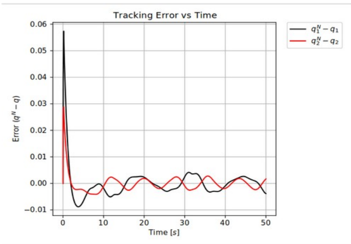

Figure 26
Trajectory tracking error of the adaptive SMC controller with Steffensen's accelerator, and without noise in the case of weak coupling

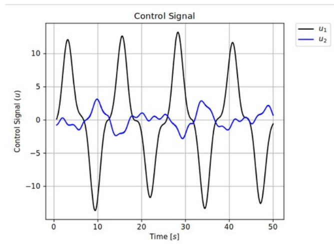

Figure 27
The control forces of the adaptive SMC controller controller with Steffensens accelerator, and without noise in the case of weak coupling

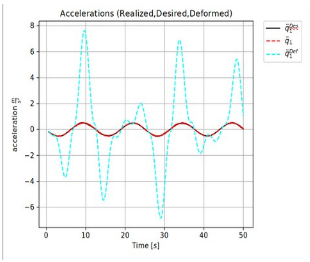

Figure 28
The $\ddot{q}_1(t)$ second-order derivative in the adaptive controller with Steffensen's accelerator, and simulated noise in the case of weak coupling

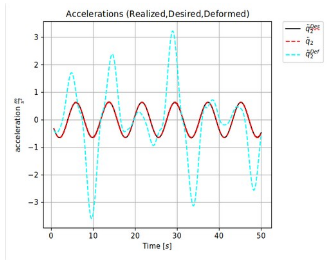

Figure 29
The $\ddot{q}_2(t)$ second-order in the adaptive SMC SMC with Steffensens accelerator, and without without noise in the case of weak coupling

Finally, by switching on the noise simulation in Fig. 30 it can be seen that though the trajectory tracking precision to some extent was corrupted, the controllers remained stable. In Fig. 31 it can be well observed that the reduced necessary control force lead to quite bad signal to noise ratio: the noise content completely hides the signal.

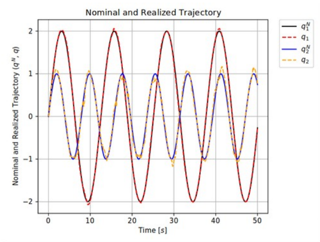

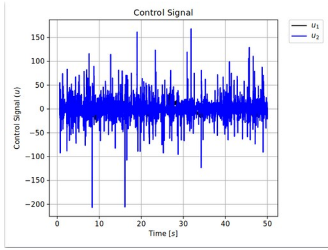

Figure 30

Trajectory tracking of the adaptive SMC controller with Steffensen, and $\sigma = 5 \times 10^{-7}$ noise the case of weak coupling

Figure 31

The control forces of the adaptive SMC controller with Steffensen, and with noise of $\sigma = 5 \times 10^{-7}$ in in the case of weak coupling

To the question what can be done for improving the situation within FPI-based adaptive SMC control framework the answer is: further reduction the cycle time δt (that in the same time is the discrete time resolution of the Euler integration in the computations). Because during one digital cycle only one step of adaptive deformation can be done, reduction of the cycle time allows more adaptive steps during unit time, i.e., it accelerates the speed of the process of adaptation. The same parameter setting yielded stable results for $\delta t = 0.5 \cdot 10^{-3}$ [s]. Figures 32, 33, and 34 testify that quality of tracking became almost as good as in the noise-free case. Figure 35 shows drastic improvement in the reduction of the signal to noise ratio of the control force and that the control forces went back to the order of magnitude as in the noise-free case in Fig. 27. Also, the necessary extent of adaptive deformation in Figs. 35 and 36 that the signal to noise become good enough to reveal the continuous trends in the variation of these quantities.

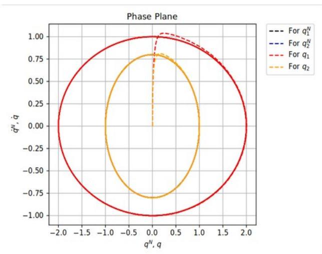

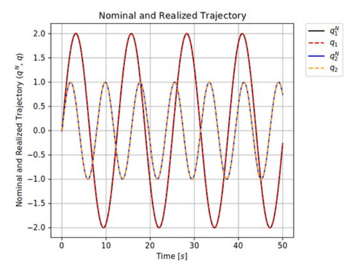

Figure 32

Phase trajectory tracking of the adaptive SMC controller with Steffensen and noise of $\sigma = 5 \times 10^{-7}$ [m] in the case of weak coupling and $\delta t = 0.5 \cdot 10^{-3}$ [s]

Figure 33

Tracjectory tracking of the adaptive SMC controller with Steffensen and noise of $\sigma = 5 \times 10^{-7}$ [m] in the case of weak coupling and $\delta t = 0.5 \cdot 10^{-3}$ [s]

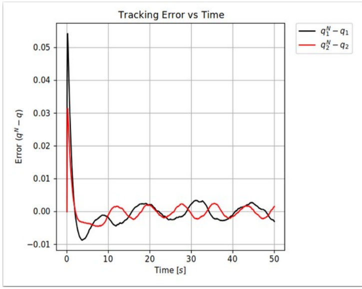

Figure 34
Trajectory tracking error of the adaptive SMC controller with Steffensen and noise of $\sigma = 5\times10^{-7}$ [m] in the case of weak coupling and $\delta t = 0.5\cdot10^{-3}$ [s]

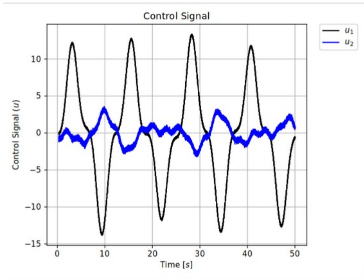

Figure 35
The control force of the adaptive SMC controller with Steffensen and noise of $\sigma = 5\times10^{-7}$ [m] in the case of weak coupling and $\delta t = 0.5\cdot10^{-3}$ [s]

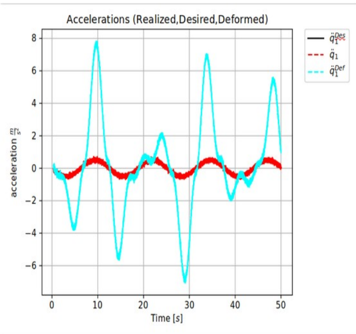

Figure 36
The $\ddot{q}_1(t)$ second-order derivative of the adaptive SMC controller with Steffensen and noise of $\sigma = 5\times10^{-7}$ [m] in the case of weak coupling and $\delta t = 0.5\cdot10^{-3}$ [s]

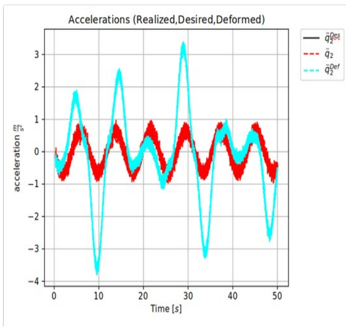

Figure 37
The $\ddot{q}_2(t)$ second-order derivativef the adaptive SMC controller with Steffensen and noise of $\sigma = 5\times10^{-7}$ [m] in the case of weak coupling and $\delta t = 0.5\cdot10^{-3}$ [s]

Conclusions

Very briefly the following conclusions can be drawn from this research:

• The various sliding mode controllers show excellent robustness against modeling imprecisions and parameter uncertainties. However, their robustness have natural limitations.

• Precision of their operation can be considerably improved by their combination with the very simple fixed point iteration-based adaptive controllers, however, the improvement is successful only if these adaptive controllers have very fast convergence.

• This fast convergence can be guaranteed by the application of Steffensen's convergence accelerator trick that successfully was generalized from single variable to multiple variable functions.

• The ultimate possibility for speeding up the convergence of the adaptation mechanism is the reduction of the cycle time of the digital controller applied. This reduction very significantly can reduce the noise-sensitivity of the control method.

In the present investigations only the integration of the simplest SMC and the simplest FPI-based adaptive control was considered. Integration of the different variants of these methods means an interesting further research area.

Acknowledgement

We acknowledge the support of this work by thr Doctoral School of Applied Informatics and Applied Mathematics of Obuda University.

References

[1] V. Utkin, "Variable structure systems with sliding modes," IEEE Transactions on Automatic Control, vol. 22, no. 2, pp. 212–222, 1977.

[2] J. Slotine and W. Li, Applied Nonlinear Control, ser. Prentice-Hall International Editions. Prentice-Hall, 1991. [Online]. Available: https://books.google.hu/books?id=HddxQgAACAAJ

[3] J. Tar, J. Bitó, L. Nádai, and J. Tenreiro Machado, "Robust Fixed Point Transformations in adaptive control using local basin of attraction," Acta Polytechnica Hungarica, vol. 6, no. 1, pp. 21–37, 2009.

[4] J. F. Steffensen, "Remarks on iteration." Scandinavian Actuarial Journal, vol. 1933, no. 1, pp. 64–72, 1933.

[5] K. Kósi and A. Awudu, "Increasing the convergence speed of robust fixed point transformaton-based adaptive control by steffensen's method in siso case," in 2022 IEEE 20th Jubilee International Symposium on Intelligent Systems and Informatics (SISY), 2022, pp. 285–290.

[6] L. Sciavicco and B. Siciliano, Modeling and control of robot manipulators. McGraw-Hill, New York, 1996.

[7] B. Armstrong, O. Khatib, and J. Burdick, "The explicit dynamic model and internal parameters of the PUMA 560 arm," in Proc. IEEE Conf. On Robotics and Automation 1986, 1986, pp. 510–518. [Online]. Available:

https://resolver.caltech.edu/CaltechAUTHORS:20190612-075818151

[8] P. Corke and B. Armstrong-Helouvry, "A search for consensus among model parameters reported for the puma 560 robot," in Proceedings of the 1994 IEEE International Conference on Robotics and Automation, vol. 2, 1994, pp. 1608–1613.

[9] S. Emelyanov, S. Korovin, and L. Levantovsky, "Higher order sliding regimes in the binary control systems," Soviet Physics, vol. 31, pp. 291–293, 1986.

[10] V. Utkin, Sliding Modes in Optimization and Control Problems. Springer Verlag, New York, 1992.

[11] L. Yang and S. Pan, "A Sliding Mode Control method for trajectory tracking control of wheeled mobile robot," Journal of Physics: Conference Series, vol. 1074, no. 1, p. 012059, 2018.

[12] J. Baek and W. Kwon, "Practical adaptive sliding-mode control approach for precise tracking of robot manipulators," Applied Sciences, vol. 10, no. 8, p. 2909, 2020.

[13] Y. Han, Y. Cheng, and G. Xu, "Trajectory tracking control of AGV based on sliding mode control with the improved reaching law," IEEE Access, vol. 7, p. 20748–20755, 2019.

[14] J. J. Slotine and S. S. Sastry, "Tracking control of non-linear systems using sliding surfaces, with application to robot manipulators," International Journal of Control, vol. 38, no. 2, pp. 465–492, 1983.

[15] S. Tokat, I. Eksin, and M. Guzelkaya, "Sliding mode control using a nonlinear time-varying sliding surface," in proceedings of the 10th Mediterranean Conference on Control and Automation-MED2002, Lisbon, Portugal, 2002, pp. 1–6.

[16] H. U. Suleiman, M. B. Mu'azu, T. A. Zarma, A. T. Salawudeen, S. Thomas, and A. A. Galadima, "Methods of chattering reduction in Sliding Mode Control: A case study of ball and plate system," in 2018 IEEE 7th International Conference on Adaptive Science & Technology (ICAST), 2018, pp. 1–8.

[17] L. Rubio, A. Ibeas, and X. Luo, "P-PI and super twisting sliding mode control schemes comparison for high-precision CNC machining," in 2016 24th Iranian Conference on Electrical Engineering (ICEE), 2016, pp. 1825–1830.

[18] P. Kachroo and M. Tomizuka, "Chattering reduction and error convergence in the sliding-mode control of a class of nonlinear systems," IEEE Transactions on Automatic Control, vol. 41, no. 7, pp. 1063–1068, 1996.

[19] P. Suryawanshi, P. Shendge, and S. Phadke, "A boundary layer sliding mode control design for chatter reduction using uncertainty and disturbance estimator," Int. J. Dynam. Control, vol. 4, p. 456–465, 2016.

[20] G. Herrmann, S. K. Spurgeon, and C. Edwards, “On sliding-mode based control via cone-shaped boundary layers,” 2002. [Online]. Available: https://api.semanticscholar.org/CorpusID:67312067

[21] A. Lyapunov, A General Task about the Stability of Motion. (in Russian). Ph.D. Thesis, University of Kazan, Tatarstan (Russia), 1892.

[22] A. Lyapunov, Stability of Motion. Academic Press, New-York and London, 1966.

[23] K. Weierstraß, “Über die analytische Darstellbarkeit sogenannter willkürlicher Functionen einer reellen Veränderlichen (About the analytical representability of so-called arbitrary functions of a real variable), Sitzungsberichte der Akademie zu Berlin (Inaugural Lecture at the Academy of Berlin, 1885), pp. 633–639, 789–805, 1885,” Mathematische Werke von Karl Weierstrass, Mayer & Müller, Berlin, vol. 3, pp. 1–37, 1903.

[24] M. Stone, “A generalized Weierstrass approximation theorem,” Math. Magazine, vol. 21, pp. 237–254, 1948.

[25] A. Kolmogorov, “On the representation of continuous functions of many variables by superposition of continuous functions of one variable and addition (in russian),” Dokl. Akad. Nauk. SSSR, vol. 114, pp. 953–956, 1957.

[26] D. Sprecher, “On the structure of continuous functions of several variables,” Trans. Amer. Math. Soc., vol. 115, pp. 340–355, 1965.

[27] G. Lorentz, Approximation of Functions. Holt, Reinhard and Winston, New York, 1965.

[28] L. Zadeh, “Fuzzy sets,” Information and Control, vol. 8, pp. 338–353, 1965.

[39] P. Menich and J. Kopják, “Optimal Fuzzy Controller, using a Genetic Algorithm for a Ball on Wheel System,” Acta Polytechnica Hungarica, vol. 20, no. 6, pp. 61–77, 2023.

[30] D. Leith and W. Leithead, “On formulating nonlinear dynamics in LPV form,” In Proc. of the 39th IEEE Conference on Decision and Control, pp. 3526–3527, 2000.

[31] B. Németh, “Providing guaranteed performances for an enhanced cruise control using robust LPV method,” Acta Polytechnica Hungarica, vol. 20, no. 7, pp. 133–152, 2023.

[32] A. Reda, R. Benotsmane, A. Bouzid, and J. Vásárhelyi, “A hybrid Machine Learning-based control strategy for autonomous driving optimization,” Acta Polytechnica Hungarica, vol. 20, no. 9, pp. 165–186, 2023.

[33] K. Weierstraß, "Über continuirliche Functionen eines reellen Arguments, die für keinen Werth des letzeren einen bestimmten Differentialquotienten besitzen, (On single variable continuous functions that nowhere are differentiable)," in: Königlich Preussichen Akademie der Wissenschaften, Mathematische Werke von Karl Weierstrass, Berlin, Germany: Mayer & Mueller, 1895, vol. 2, pp. 71–74, 1895.

[34] B. Csanádi, P. Galambos, J. K. Tar, G. Györök, and A. Serester, "A novel, abstract rotation-based fixed point transformation in adaptive control," in 2018 IEEE International Conference on Systems, Man, and Cybernetics (SMC), 2018, pp. 2577–2582.

[35] S. Banach, "Sur les opérations dans les ensembles abstraits et leur application aux équations intégrales (About the Operations in the Abstract Sets and Their Application to Integral Equations)," Fund. Math., vol. 3, pp. 133–181, 1922. [Online]. Available: http://eudml.org/doc/213289

[36] A. Dineva, J. K. Tar, A. Várkonyi-Kóczy, and V. Piuri, "Generalization of a sigmoid generated Fixed Point Transformation from SISO to MIMO systems," in 2015 IEEE 19th International Conference on Intelligent Engineering Systems (INES), 2015, pp. 135–140.

[37] B. Lantos and Z. Bodó, "High level kinematic and low level nonlinear dynamic control of unmanned ground vehicles," Acta Polytechnica Hungarica, vol. 16, no. 1, pp. 97–117, 2019.

[38] B. Varga, J. K. Tar, and R. Horváth, "Fractional order inspired iterative adaptive control," Robotica, p. 1–28, 2023.

[39] B. van der Pol, "Forced oscillations in a circuit with non-linear resistance (reception with reactive triode)," The London, Edinburgh, and Dublin Philosophical Magazine and Journal of Science, vol. 7, no. 3, pp. 65–80, 1927.